International Journal of Pharmacology

Int. J. Pharmacol. **2026**; 22(6): 50583
https://doi.org/10.31083/IJP50583

Research Article

In Vitro Study on the Effects of the Combined Use of a PD-L1 Silencing and Rituximab on Diffuse Large B-Cell Lymphoma

Zhiping Ma[1], Xuelian Pang[1], Wenli Cui[1], Wei Zhang[1,*]

[1]Department of Pathology, The First Affiliated Hospital of Xinjiang Medical University, 830054 Urumqi, Xinjiang, China
*Correspondence: zhangwei20241113@126.com (Wei Zhang)

Academic Editor: Mehmet Ozaslan
Submitted: 1 February 2026 Revised: 10 April 2026 Accepted: 22 April 2026 Published: 26 October 2026

Abstract

Background: The inhibitory immune checkpoint molecule programmed cell death ligand 1 (PD-L1) represents a promising therapeutic target for lymphoid malignancies. Moreover, PD-L1 expression in the tumor microenvironment correlates with tumor progression. **Methods:** This study used human diffuse large B cell lymphoma (DLBCL) cell lines SU-DHL-2 and SU-DHL-6. These cell lines were treated with either a PD-L1 smart silencer RNA (ssiPD-L1) or rituximab to evaluate antitumor effects by assessing cell viability, migration, and invasion. Flow cytometry was employed to assess cell apoptosis, and potential signaling pathways were examined using quantitative polymerase chain reaction (qPCR) and Western blot analyses. **Results:** Treatment with ssiPD-L1 significantly reduced PD-L1 expression, compared with the normal control smart silencer (ssiNC). Cell viability, migration, and invasion were significantly decreased after treatment with ssiPD-L1 or rituximab compared with control cells, with more pronounced effects observed after combination therapy. Administration of ssiPD-L1 or rituximab significantly increased the proportion of apoptotic and necrotic cells, while the proportion of proliferating cells was significantly reduced, again with stronger effects after combined treatment. Expression of PD-L1, the NF-κB, p-P65, C-X-C chemokine receptor type 4 (CXCR4), and B-cell lymphoma 2 (BCL-2) was significantly reduced after ssiPD-L1 or rituximab treatment. However, Bax expression, an apoptosis marker, was significantly increased in ssiPD-L1- and rituximab-treated cells, with the effect more pronounced in co-treated cells. **Conclusion:** Combined PD-L1 silencing and rituximab treatment inhibits DLBCL progression *in vitro* by promoting apoptosis and modulating NF-κB–related signaling pathways.

Keywords: diffuse large B-cell lymphoma; PD-L1; Rituximab; NF-κB; apoptosis

1. Introduction

Diffuse large B-cell lymphoma (DLBCL) is characterized by robust aggressiveness, high-grade malignancy, and a poor prognosis, thereby posing serious threats to patients' lives [1,2]. The standard R-CHOP regimen, which includes rituximab (a monoclonal anti-CD20 antibody), cyclophosphamide, doxorubicin, vincristine, and prednisone, provides substantial clinical benefit for most patients with diffuse large B-cell lymphoma [3,4,5,6]. However, some patients may still experience relapse or develop refractory disease due to drug resistance, indicating that this therapeutic approach is not universally effective in clinical practice. Therefore, identifying more effective therapeutic strategies and combining them with the R-CHOP regimen is critical for improving the long-term prognosis of patients with DLBCL.

Recent advances in immunology have established immunotherapy as a viable treatment option for various cancers. The tumor microenvironment is recognized as a critical determinant of lymphoma initiation, progression, recurrence, and drug resistance [7,8]. Within this milieu, programmed cell death ligand 1 (PD-L1) and its receptor programmed cell death 1 (PD-1/CD279) function as inhibitory immune checkpoint molecules that drive the production of immunosuppressive cytokines, thereby dampening antitumor immunity [9]. A retrospective study demonstrated a close correlation between PD-L1 expression and overall survival in patients with DLBCL, with high PD-L1 expression associated with poorer survival outcomes [10]. Moreover, PD-L1 overexpression has been identified as a common feature in more aggressive DLBCL subtypes, indicating that the PD-1/PD-L1 axis may be a potential therapeutic target in DLBCL immunotherapy and a contributor to its aggressive progression [11]. Preclinical and clinical trials have further confirmed the efficacy of nivolumab and pembrolizumab against DLBCL [12,13,14].

The PD-1/PD-L1 axis has been implicated in the development of chemoresistance to standard CHOP regimens in DLBCL cell lines, potentially through the regulation of phosphatidylinositol 3-kinase-protein kinase B (PI3K-AKT), apoptosis-related, and nuclear factor kappa-B (NF-κB) signaling pathways [15,16,17]. Furthermore, aberrant activation of NF-κB signaling has been shown to suppress apoptosis while promoting cancer cell proliferation, migration, invasion, angiogenesis, and epithelial-mesenchymal transition (EMT), primarily through the upregulation of vascular endothelial growth factor (VEGF), matrix metalloproteinases (MMPs), and C-X-C chemokine receptor type 4 (CXCR4) [18,19]. These observations underscore the criti-

Copyright: © 2026 The Author(s). Published by IMR Press.
This is an open access article under the CC BY 4.0 license.

Publisher's Note: IMR Press stays neutral with regard to jurisdictional claims in published maps and institutional affiliations.

cal roles of both the PD-1/PD-L1 axis and NF-κB signaling in DLBCL progression and the acquisition of chemoresistance.

However, the mechanistic relationship between the PD-1/PD-L1 axis and apoptosis-related or NF-κB signaling pathways during DLBCL pathogenesis remains poorly defined. In this study, we investigated the functional roles of a PD-L1 smart silencer in combination with rituximab in modulating DLBCL behaviors *in vitro*. Our findings provide a theoretical foundation for the development of novel therapeutic strategies targeting both rituximab and PD-L1 pathway blockade in DLBCL.

2. Materials and Methods

2.1 Cell Lines and Culture Conditions

The human DLBCL cell lines SU-DHL-2 (activated B-cell-like (ABC) subtype) and SU-DHL-6 (germinal center B-cell-like (GCB) subtype) were provided as typical suspension cells by Key-Gen Biotechnology Company (Nanjing, China) and cultured in Roswell Park Memorial Institute (RPMI) 1640 medium (Gibco, Thermo Fisher Scientific, Waltham, MA, USA), supplemented with 10% fetal bovine serum (FBS; Gibco) and 1% penicillin and streptomycin (Gibco), cultivate at 37 ℃ and 5% CO_2. Our PD-L1 smart silencer (ssiPD-L1) was a mixture of three small interfering RNAs (siRNAs) and three antisense oligonucleotides (ASOs) synthesized by RiboBio (Guangzhou, China). The ssiRNA sequences for PD-L1 were as follows: GACAAGCAGTGACCATCAA, GATATTTGCTGTCTTTATA, GCTGTCTTTATATTCATGA, ATGACCTACTGGCATTTGCT, CCCATACAACAAAATCAACC, and GTCACCTCTGAACATGAACT. Furthermore, we employed the silencer mixture to inhibit PD-L1 expression in these cells; normal control small silencer (ssiNC) was also applied by Ribobio (Guangzhou, China) as the control. Cells were transfected with ssiNC and ssiPD-L1 using Lipofectamine 2000 (Thermo Fisher, Waltham, MA, USA) and then treated with different concentrations of the anti-CD20 chimeric monoclonal antibody rituximab (Meilun Biotechnology Co., Ltd., Dalian, China). All cell lines were validated by STR profiling and tested negative for mycoplasma.

2.2 Cell Counting Kit-8 (CCK-8) Assay

SU-DHL-2 and SU-DHL-6 cells were seeded in 96-well plates at a density of 2×10^4/mL (100 µL/well). Following transfected with ssiNC or ssiPD-L1, the cells were treated with increasing concentrations of rituximab (0, 1.0, 2.5, 5.0, 7.5, 10.0, and 15.0 µg/mL). Each concentration was tested in triplicate. After 24 or 48 h of treatment, 10 µL of CCK-8 solution (Beyotime Institute of Biotechnology, Jiangsu, China) was added to each well, and the plates were incubated at 37 °C for 4 h. Cell viability was then assessed by measuring absorbance at 450 nm.

2.3 Cellular Migration Assay

To evaluate cell migration, 24-well Transwell plates (Corning Incorporated, Corning, NY, USA) were pre-coated with 100 µL of Matrigel (300 µg/mL) for 8 h. Following transfection with ssiNC or ssiPD-L1 and subsequent rituximab treatment, cells were harvested and resuspended at 5×10^5 cells/mL, after which 200 µL aliquots were seeded into the upper chambers. Following 24 h of incubation, cells that had migrated to the lower chambers were collected, transferred to 96-well plates, and incubated for an additional 4 h with 20 µL of CCK-8 solution (Beyotime). Absorbance at 450 nm was then measured to quantify the migratory capacity.

2.4 Cellular Invasion Assay

To assess invasive capacity, 24-well Transwell plates (Corning) were pre-coated with 100 µL of Matrigel (300 µg/mL) for 8 h. Following transfection with ssiNC or ssiPD-L1 and rituximab treatment, cells were resuspended at 5×10^5 cells/mL, and 200 µL aliquots were seeded into the upper chambers. After 24 h of incubation, cells that had invaded through the Matrigel were collected, transferred to 96-well plates, and incubated for 4 h with 20 µL of CCK-8 solution (Beyotime). Absorbance at 450 nm was then measured to quantify invasive activity.

2.5 Cellular Apoptosis Analysis

Following treatment for 24 h, SU-DHL-2 and SU-DHL-6 cells were harvested through trypsinization. Apoptosis was assessed using the Annexin Fluorescein isothiocyanate labeled membrane associated protein V (V-FITC)/propidium iodide (PI) apoptosis detection kit (Key-Gen) according to the manufacturer's instructions. Briefly, cells were resuspended in 500 µL of binding buffer, stained with 5 µL of Annexin V-FITC, and then incubated with 5 µL of PI for 15 min in the dark prior to flow cytometric analysis. Data were analyzed using FlowJo software v10.8 (BD Corp., Franklin Lakes, NJ, USA). Doublets were excluded, and apoptosis was analyzed by gating on viable cells based on FMO controls.

2.6 Quantitative Real-Time Polymerase Chain Reaction (qRT-PCR) Analysis

Total RNA was isolated from SU-DHL-2 and SU-DHL-6 cells following treatment using TRIzol reagent (Ambion Biotechnology, Austin, TX, USA). First-strand cDNA was synthesized from the resulting RNA using a PrimeScript RT reagent kit (Vazyme Biotechnology Co., Ltd., Nanjing, China) according to the manufacturer's protocol. qRT-PCR was performed using SYBR Premix Ex Taq II (Vazyme, Nanjing, China) on an iQ6 gradient real-time PCR detection system CFX96 (Bio-Rad, Hercules, CA, USA). The thermal cycling conditions consisted of an initial denaturation at 95 °C for 10 min, followed by 40 cycles of 95 °C for 15 s and 60 °C for 60 s. Melting curve

Table 1. Primers used in qRT-PCR analysis.

Gene name	Forward primer sequence (5′ →3′)	Reverse primer sequence (5′→3′)	PCR products
PD-L1	ATGTCAGGCTGAGGGCTAC	GGATGTGCCAGAGGTAGTT	240 bp
P65	CAGCGTGGGGACTACGACCTGAATG	GGGGCACGATTGTCAAAGATGGGAT	125 bp
CXCR4	ATCTGTGACCGCTTCTACCC	CGATGCTGATCCCAATGTAG	232 bp
Bax	AAGAAGCTGAGCGAGTGTCT	GTTCTGATCAGTTCCGGCAC	236 bp
BCL-2	GCCTTCTTTGAGTTCGGTGG	GAAATCAAACAGAGGCCGCA	192 bp
GAPDH	TCAAGAAGGTGGTGAAGCAGG	TCAAAGGTGGAGGAGTGGGT	115 bp

PD-L1, programmed cell death ligand 1; P65, nuclear factor NF-kappa-B p65 subunit; CXCR4, C-X-C chemokine receptor type 4; BCL-2, B-cell lymphoma 2; Bax, Bcl-2 associated X protein; GAPDH, glyceraldehyde-3-phosphate dehydrogenase.

analysis was conducted to verify the specificity of amplification and to rule out primer-dimer formation or secondary products. Relative gene expression levels were calculated using the $2^{-\triangle\triangle Ct}$ method, with GAPDH serving as the internal reference gene. All primers used in this study were synthesized by Tsingke Biotechnology Company (Beijing, China) and are listed in Table 1.

2.7 Western-Blot Analysis

Total protein was extracted from treated SU-DHL-2 and SU-DHL-6 cells using radioimmunoprecipitation assay (RIPA) lysis buffer (Beyotime, Shanghai, China). Protein concentrations were determined using a bicinchoninic acid (BCA) protein assay kit (Beyotime), and 40 µg of protein per sample was used for subsequent analysis. Equal amounts of protein were separated by 10% sodium dodecyl sulfate-polyacrylamide gel electrophoresis (SDS-PAGE) and transferred onto polyvinylidene difluoride (PVDF) membranes (Merck-Millipore, Darmstadt, Germany). Membranes were blocked with 5% non-fat dry milk in Tris-buffered saline containing 0.1% Tween 20 (TBST) for 1 h at room temperature and then incubated overnight at 4 °C with primary antibodies targeting PD-L1 (1:1000; Abcam, Cambridge, MA, USA), P65 (mouse monoclonal, 1:1000; Zen-Bio, Chengdu, China), phosphorylated P65 (p-P65, rabbit polyclonal, 1:1000; Zen-Bio), BCL-2 (mouse monoclonal, 1:1000; Abcam), Bax (mouse monoclonal, 1:1000; Cusabio, Wuhan, China), CXCR4 (rabbit polyclonal, 1:1000; Abcam), or GAPDH (rabbit monoclonal, 1:1000; Abcam). After washing with TBST, membranes were incubated with horseradish peroxidase (HRP)-conjugated secondary antibodies (1:5000; Boster, Wuhan, China) for 1 h at 37 °C. Protein bands were visualized and quantified using Fusion software (Vilber, Paris, France), and relative protein expression levels were normalized to GAPDH.

2.8 Statistical Analysis

Statistical analysis was performed using SPSS 20.0 (IBM, Stanford, CA, USA), and graphical representations were generated with GraphPad Prism 10.0 (GraphPad Software, San Diego, CA, USA). All data are presented as the mean ± standard deviation (SD). Comparisons between two groups were evaluated using Student's *t*-test, while comparisons among multiple groups were analyzed by repeated measures ANOVA. A p value < 0.05 was considered statistically significant, with significance levels denoted as *(p < 0.05), **(p < 0.01), and ***(p < 0.001).

3. Results

3.1 Determination of Rituximab Concentrations and Confirmation of PD-L1 Interference

Compared with the control cells, the cellular viability of SU-DHL-2 cell lines was 80.8% at a rituximab concentration of 10 µg/mL and decreased to 73.61% at a concentration of 15 µg/mL (Fig. 1A). Therefore, 10 µg/mL rituximab was the optimal concentration we used for SU-DHL-2 cell lines in the subsequent study. Regarding SU-DHL-6 cell lines, cellular viability was 75.34% at a concentration of 5 µg/mL and further declined to 69.45% and 60.21%, respectively, at concentrations of 7.5 µg/mL and 10 µg/mL (Fig. 1B). Thus, 5 µg/mL rituximab was the suitable concentration for SU-DHL-6 cell lines, and this concentration was applied to the following studies. Fig. 1C,D show the morphology of two cell lines treated with rituximab.

The interference with PD-L1 employing a small silencer was confirmed through qRT-PCR analysis. Compared with ssiNC, PD-L1 expression was significantly reduced after treatment with ssiPD-L1 in both cell lines, and the inhibition rates were 44.3% and 56.5% for SU-DHL-2 and SU-DHL-6 cell lines, respectively (Fig. 1E,F). The above data suggest successful interference with PD-L1 by the small silencer mixture, which was then used for *in vitro* analysis.

3.2 Proliferative, Migratory, and Invasive Capabilities of Differentially Treated Cell Lines

Compared with control cells, cellular viabilities significantly declined after separate treatment of SU-DHL-2 cell lines with ssiPD-L1 and 10 µg/mL rituximab, which were 81.25% and 79.08%, respectively (p < 0.05). Intriguingly, the combined use of ssiPD-L1 and rituximab significantly diminished cellular viability to only 55.43% (Fig. 2A). Concerning SU-DHL-6 cell lines, cellular viability

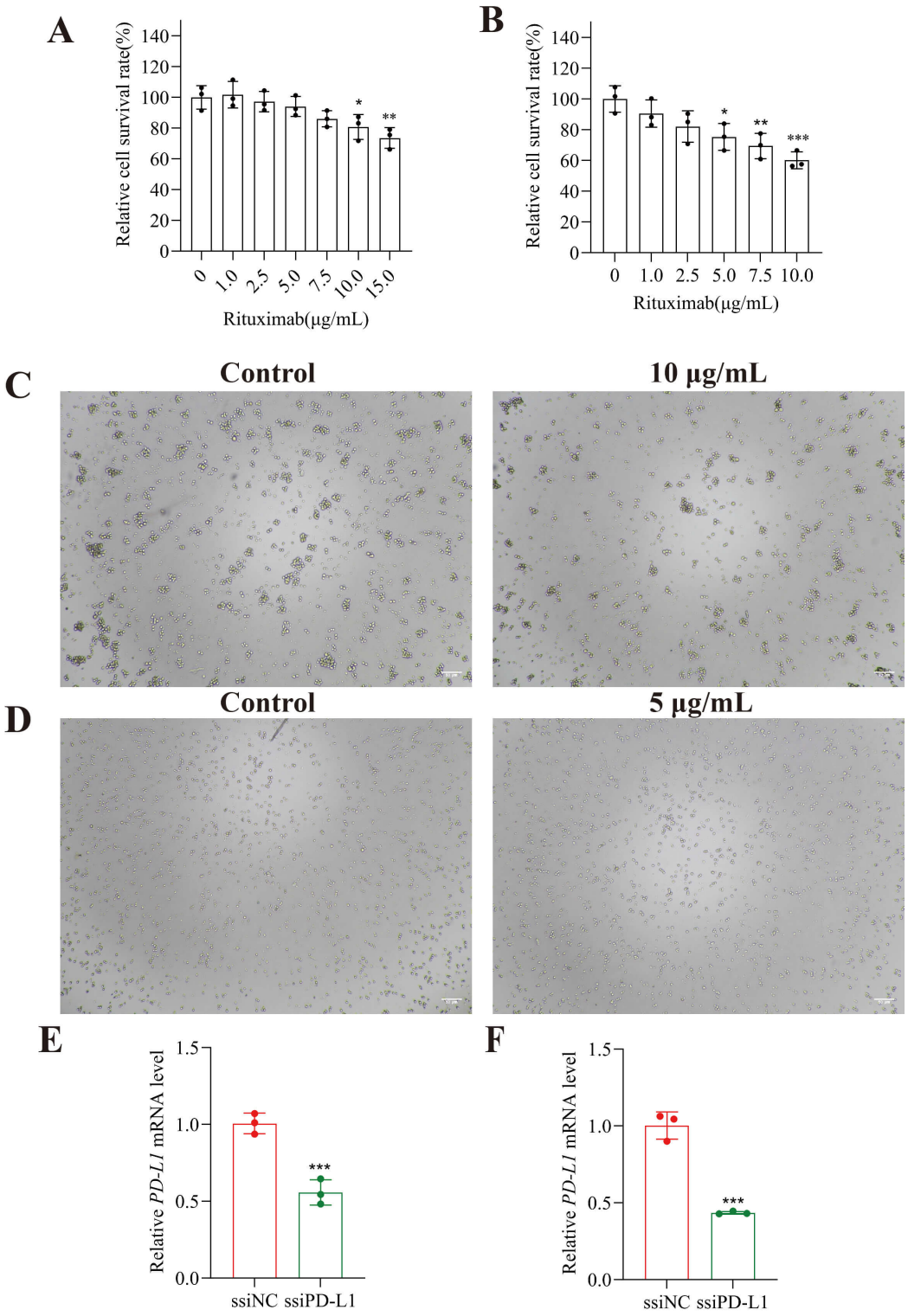


Fig. 1. Determination of rituximab concentration and confirmation of PD-L1 interference in SU-DHL-2 and SU-DHL-6 cell lines. Dynamic changes in cellular viability in SU-DHL-2 (A) and SU-DHL-6 (B) cell lines after treatment with rituximab. $^{*}p < 0.05$, $^{**}p < 0.01$, $^{***}p < 0.001$ compared with the control group. Representative morphological images of SU-DHL-2 (C) and SU-DHL-6 (D) cell lines after treatment with or without rituximab (scale bar, 50 μm). PD-L1 mRNA expression was evaluated through qRT-PCR analysis to confirm PD-L1 interference in SU-DHL-2 (E) and SU-DHL-6 (F) cell lines. Data are presented as mean ± SD, n = 3/group. $^{***}p < 0.001$ compared with the normal control small silencer (ssiNC) group. qRT-PCR, quantitative real-time polymerase chain reaction; SD, standard deviation.

also significantly dropped after the combined use of ssiPD-L1 and rituximab relative to their separate use, with the latter viabilities showing means of 80.01% and 75.04% in ssiPD-L1-treated and 5 μg/mL rituximab-treated SU-DHL-6 cell lines, respectively. Combined use attenuated cellular viability further to 49.86% (Fig. 2B), suggesting that the combined use of PD-L1 with rituximab exerted an inhibitory effect on cellular proliferation.

SU-DHL-2 and SU-DHL-6 are suspension cell lines, and we therefore determined their migratory capability with a CCK-8 assay. Our results revealed that treatment with ssiPD-L1 or rituximab caused a significant diminution in cellular migration of SU-DHL-2 and SU-DHL-6 cell lines compared with control cells ($p < 0.05$; Fig. 2C,D). Moreover, their combined use resulted in a further significant decline in the migratory ability of these cell lines, suggesting obvious inhibitory effects of ssiPD-L1 and rituximab on the migration of SU-DHL-2 and SU-DHL-6 cells.

As tumor cells exhibit varying degrees of invasive potential, we next assessed the invasive capacity of SU-DHL-2 and SU-DHL-6 cells following different treatments. Both cell lines demonstrated pronounced invasiveness under control conditions, which was significantly suppressed by treatment with either ssiPD-L1 or rituximab alone ($p < 0.05$; Fig. 2E,F). Notably, combined treatment with ssiPD-L1 and rituximab resulted in an even greater reduction in invasive capacity.

3.3 Effects of ssiPD-L1 and Rituximab on Cellular Apoptosis

Cellular apoptosis may be affected after the use of ssiPD-L1 and/or rituximab. Compared with the control cells, both early and late cellular apoptosis were significantly augmented after applying ssiPD-L1 or rituximab to either cell line and made even more obvious in the cell lines that were simultaneously treated with ssiPD-L1 and rituximab ($p < 0.05$; Fig. 3A–D).

3.4 Mechanisms Related to Inhibitory Effects of the Combined Application of ssiPD-L1 and Rituximab on DLBCL Cell Lines

Compared with ssiNC-treated cell lines, PD-L1 mRNA and protein expression levels in both SU-DHL-2 and SU-DHL-6 cell lines were significantly reduced after treatment with ssiPD-L1 and rituximab ($p < 0.05$), becoming even more profound with their combined use ($p < 0.01$) (Fig. 4A,B, Fig. 5A,B). The NF-κB-signaling pathway and apoptosis may play significant roles in the inhibitory effects of ssiPD-L1 or rituximab on DLBCL cells. Thus, we employed the representative NF-κB-signaling pathway markers P65 and CXCR4, the apoptosis-related marker Bax, and the anti-apoptotic marker BCL-2 in SU-DHL-2 and SU-DHL-6 cell lines, and we evaluated them via qRT-PCR and western-blot analysis (Figs. 4A,B, Fig. 5A–D). As expected, expression of P65, CXCR4, and BCL-2 mRNA in these cell lines was significantly decreased after the application of ssiPD-L1 or rituximab compared with ssiNC-treated cells ($p < 0.05$). Interestingly, however, the combined administration of ssiPD-L1 and rituximab led to a greater decline in the expression of the above markers ($p < 0.05$). Nevertheless, compared with the control cells, expression of the apoptotic marker Bax mRNA significantly rose in ssiPD-L1/rituximab-treated cell lines ($p < 0.05$) and was also heightened in ssiPD-L1 and rituximab co-treated cells ($p < 0.01$). Western-blot analysis revealed that there was no difference in total P65 protein expression between groups ($p > 0.05$). In contrast, treatment with ssiPD-L1 or rituximab caused diminished expression of p-P65, CXCR4, and BCL-2 protein ($p < 0.05$), and the reduced expression was greater in ssiPD-L1 and rituximab co-treated cells ($p < 0.01$). However, Bax protein expression was inconsistent with the above marker proteins in that the application of ssiPD-L1 or rituximab resulted in elevated expression of Bax protein in SU-DHL-2 and SU-DHL-6 cell lines ($p < 0.05$), and their combined application showed even greater effects on the Bax elevation ($p < 0.01$). The above results strongly suggest that ssiPD-L1 and rituximab exerted significant inhibitory effects on DLBCL cell lines and that this phenomenon was a complex process that may be regulated through the NF-κB-signal-transduction pathway and apoptosis.

4. Discussion

It has been previously demonstrated that 30–40% of DLBCL patients fail to benefit from standard therapy and that immunotherapy using immune-checkpoint inhibitors produced successful treatment and significantly improved overall survival in patients with various cancers [20,21]. Specifically, PD-1 and PD-L1 were significantly enhanced in the tumor microenvironment, and expression levels constituted an indicator of poor prognosis and were closely correlated with patients' treatment response [22,23,24]. Therefore, the use of PD-1/PD-L1-pathway inhibitors comprises an attractive regimen to treat malignancies. In lymphoid malignancies, PD-L1 was elevated and correlated with clinical and pathologic characteristics, suggesting the potential therapeutic significance of this immune-checkpoint inhibitor [25]. Investigating the roles of PD-L1 and its possible underlying mechanisms of action in the development of DLBCL may provide a valuable reference to clinicians who wish to explore optimal treatment modalities and resolve potential drug resistance.

It is widely recognized that immune-checkpoint inhibitors impair cellular activation and attenuate cytokine production, promoting the rapid growth of cancer cells and thus involving in anti-tumor immune responses [26,27]. We employed two types of human DLBCL cell lines (SU-DHL-2 and SU-DHL-6) in the present study to clarify the actions of immune inhibitors on DLBCL development *in vitro* by treating the cells with ssiPD-L1 and the anti-CD20 mono-

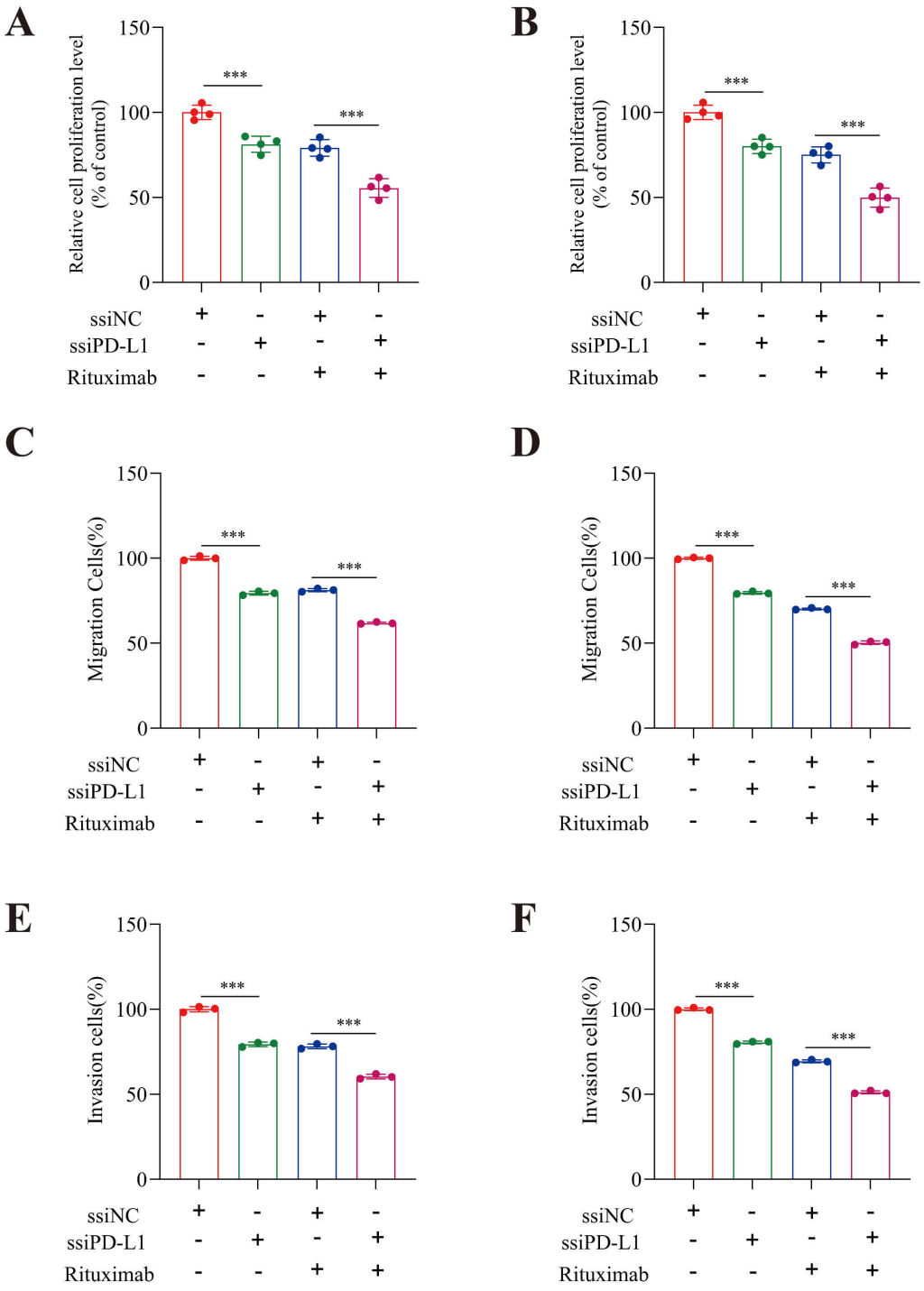


Fig. 2. Effects of ssiPD-L1 and rituximab on the proliferation, migration, and invasion abilities of SU-DHL-2 and SU-DHL-6 cell lines. Quantitative analysis of proliferation capacity of SU-DHL-2 (A) and SU-DHL-6 (B) cell lines after combined treatment with ssiPD-L1 and/or rituximab. Quantitative analysis of the migration ability of SU-DHL-2 (C) and SU-DHL-6 (D) cell lines after combined treatment with ssiPD-L1 and/or rituximab. Quantitative analysis of the invasion ability of SU-DHL-2 (E) and SU-DHL-6 (F) cell lines after combined treatment with ssiPD-L1 and/or rituximab. Data are presented as mean ± SD, n ≥ 3 per group ($^{***}p < 0.001$). ssiPD-L1, PD-L1 smart silencer.

clonal antibody rituximab. We observed that treating the cell lines with ssiPD-L1 induced a significant loss of PD-L1 expression relative to the control cells. Moreover, our results revealed that the separate or combined use of ssiPD-L1 or rituximab resulted in a marked reduction in cellular viability and migratory and invasive capabilities, which

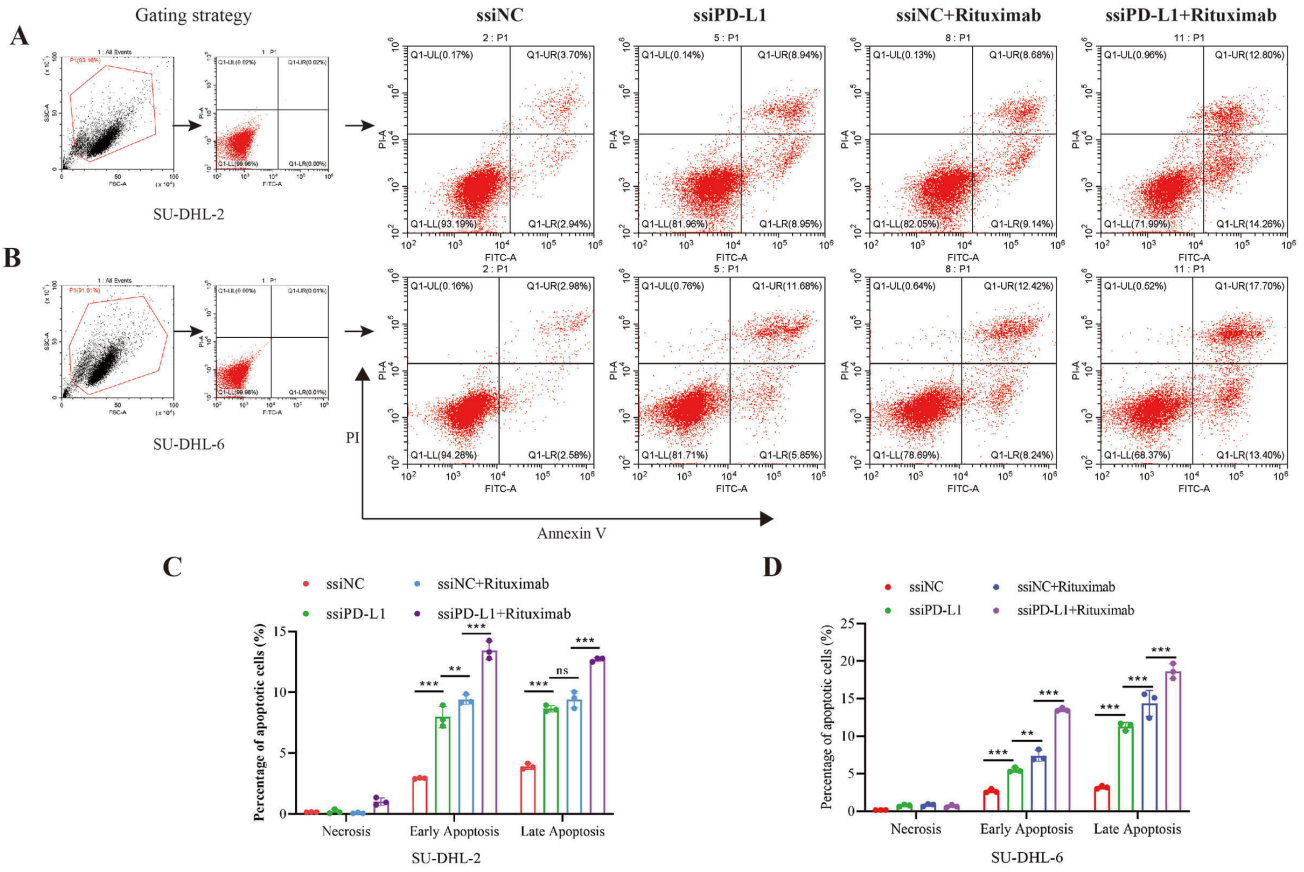


Fig. 3. Effects of ssiPD-L1 and rituximab on cellular apoptosis of SU-DHL-2 and SU-DHL-6 cell lines. Flow cytometry was used to detect cellular apoptosis in SU-DHL-2 (A) and SU-DHL-6 (B) cell lines after combined treatment with ssiPD-L1 and/or rituximab. Gates were set based on fluorescence minus one controls. Numbers indicate the percentage of cells in each quadrant. Quantitative analysis identified the alterations in cellular apoptosis in SU-DHL-2 (C) and SU-DHL-6 (D) cell lines after combined treatment with ssiPD-L1 and/or rituximab. Data are presented as mean ± SD, n = 3 per group ($^{**}p < 0.01$, $^{***}p < 0.001$, ns: no significant difference).

were made more evident by their combined use. These results were consistent with previous studies where immune-checkpoint inhibitors appeared to exert their therapeutic effects by attenuating the migratory and aggressive characteristics of cancer cells [28,29]. In addition, administration of ssiPD-L1 or rituximab led to a significant increase in cellular apoptosis, which was also heightened after their combined use. However, cellular proliferation was significantly reduced after treating the lines with ssiPD-L1 or rituximab, and this effect was exacerbated after their combined use. Apoptotic analysis via flow cytometry was also in agreement with the above results in that cellular necrosis and apoptosis were significantly augmented after applying ssiPD-L1 or rituximab to both cell lines, and the increase was enhanced with their combined use. However, treatment with ssiPD-L1 or/and rituximab also resulted in a decline in cell number, and thus, the alterations in the migratory and invasive capacities of DLBCL cell lines may have been attributed to the reduced cell number after treatment with ssiPD-L1 or/and rituximab. Collectively, the aforementioned results suggest that immune-check blockade as represented by PD-L1 and CD20 inhibition hindered the proliferative, migratory, and invasive capabilities of DLBCL cell lines *in vitro* and that these effects were intimately associated with the cellular necrosis and apoptosis induced by immune inhibitors.

Extensive pathways may exist that are involved in the anti-tumor immune responses in immune-checkpoint blockade, including the inhibition of pro-inflammatory pathways and the reduction in tumor antigens and promotion of suppressive cytokines and co-inhibitors—eventually orchestrating an immunosuppressive microenvironment [30,31,32]. As one of the significant pro-inflammatory pathways, activation of NF-κB signaling reflects vital significance in the development of lymphoma malignancies by enhancing the expression of VEGF and CXCR4 in a cancerous microenvironment [17,19,33]. Importantly, the present study revealed that mRNA and protein expression levels for NF-κB signaling-related markers—including PD-L1, P65, and CXCR4—were significantly reduced after treatment of either cell line, with ssiPD-L1 or rituximab, and that this reduction was exacerbated with their combined use. This

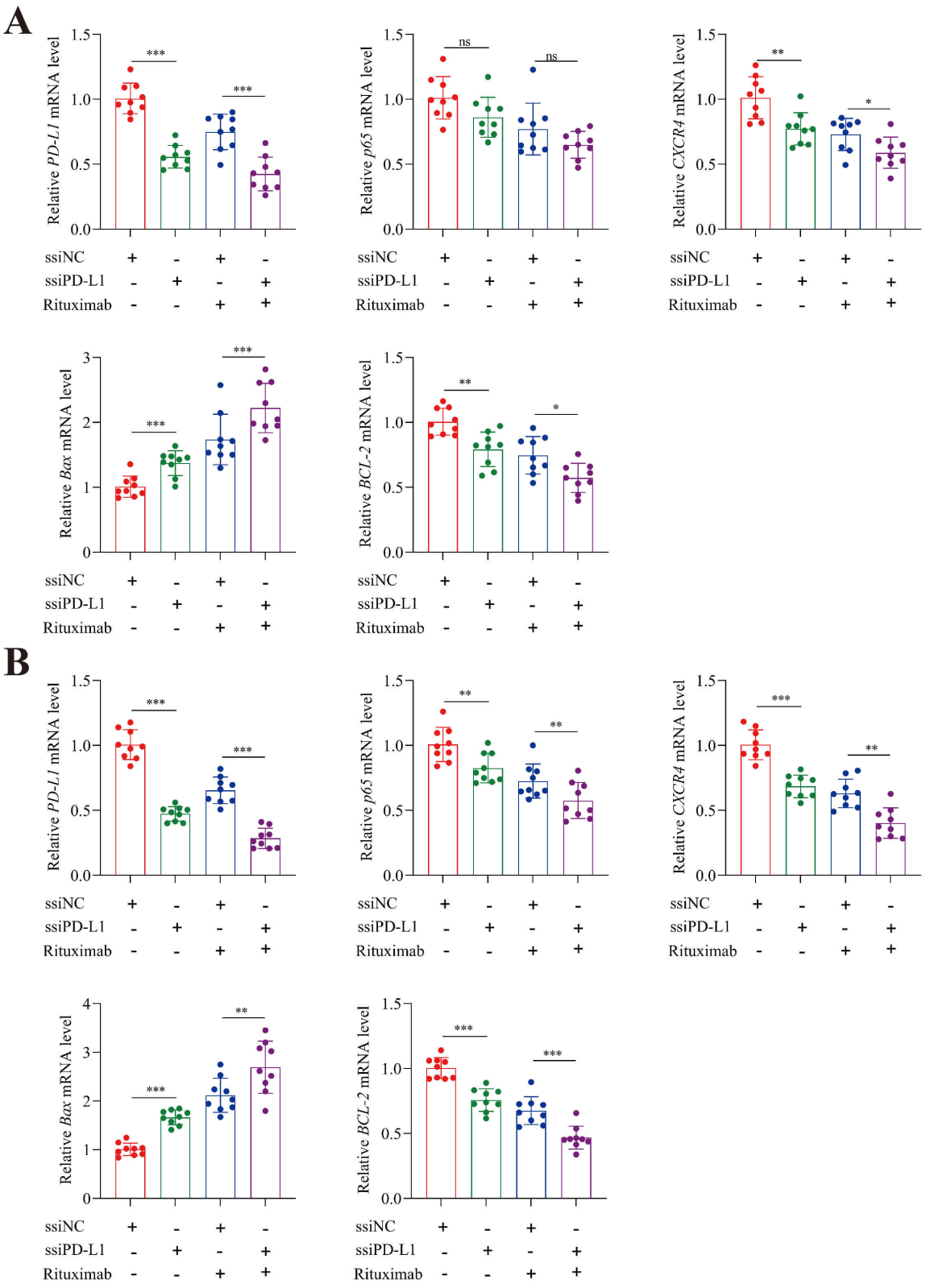


Fig. 4. Quantitative analysis was used to detect the expression levels of mechanistic markers at transcriptional level in SU-DHL-2, SU-DHL-6 cell lines after treatment with ssiPD-L1 and rituximab. qRT-PCR analysis was used to detect PD-L1, P65, CXCR4, Bax, and BCL-2 mRNA expression in SU-DHL-2 (A) and SU-DHL-6 cell lines (B). Data are presented as mean ± SD, n = 9 per group ($^{*}p < 0.05$, $^{**}p < 0.01$, $^{***}p < 0.001$, ns: no significant difference).

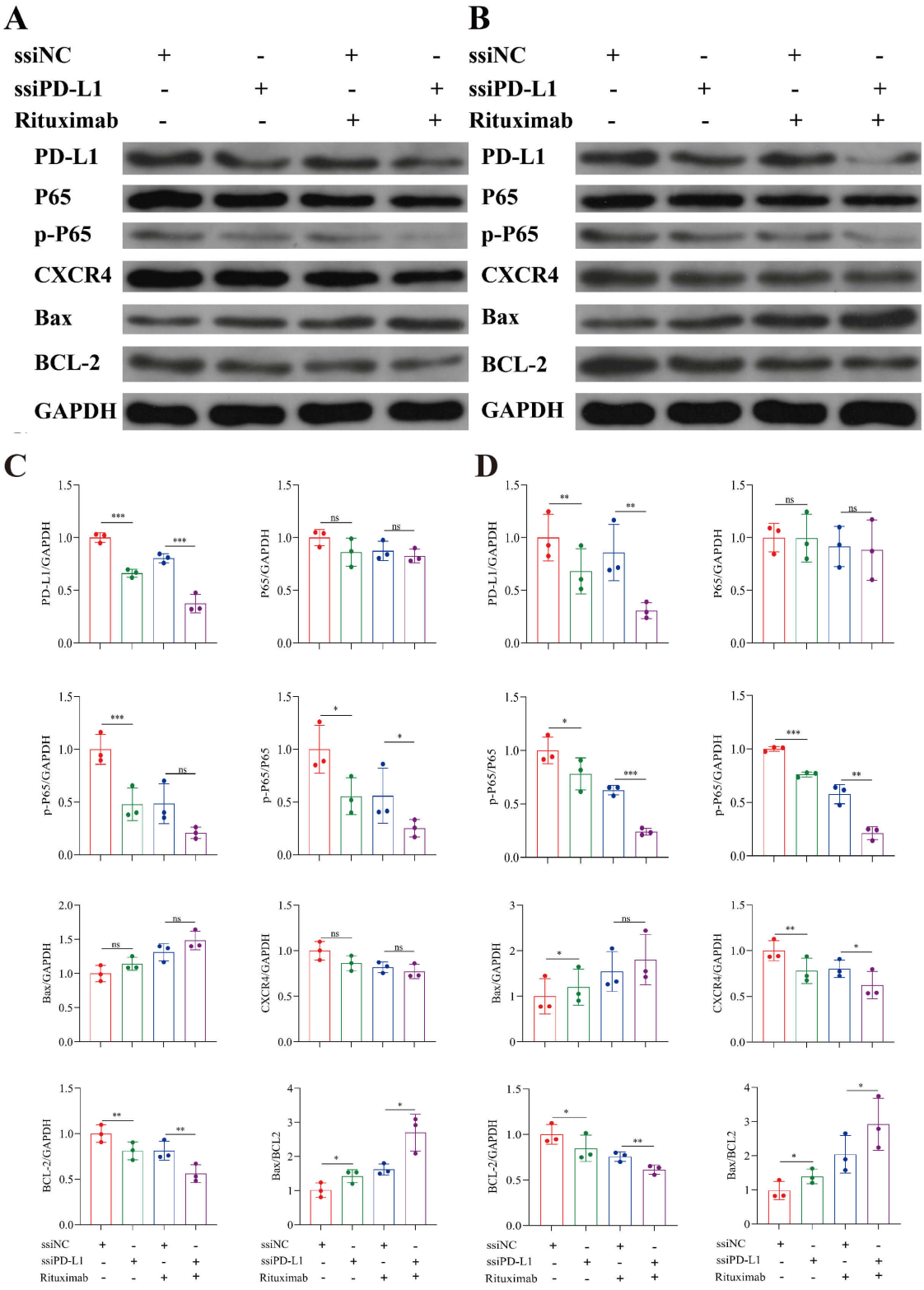


Fig. 5. Quantitative analysis was applied to measure the expression levels of mechanistic markers at protein level in SU-DHL-2 and SU-DHL-6 cell lines after treatment with ssiPD-L1 and rituximab. Western blotting analysis was used to detect PD-L1, P65, p-P65, CXCR4, Bax, and BCL-2 protein expression in SU-DHL-2 (A) and SU-DHL-6 cell lines (B). (C) Statistics of protein expression data in figure A. (D) Statistics of protein expression data in figure B. Data are presented as mean ± SD, n = 3 per group ($^{*}p < 0.05$, $^{**}p < 0.01$, $^{***}p < 0.001$, ns: no significant difference). p-P65, phosphorylated P65.

suggests that NF-κB signaling may play a crucial role in the immune-blockade process in DLBCL. NF-κB signaling-related markers represent a major link between cancer and inflammation, and aberrant activation of this signaling pathway exerts significant promoting effects on some malignancies by affecting the cellular functions of cancer cells (including proliferation, migration, and invasion). However, how this pathway exerts its effects remains unclear and needs to be further explored in future studies [34,35]. Moreover, expression of the apoptosis-related marker Bax was significantly upregulated after treatment with ssiPD-L1 or rituximab, and the expression level of the anti-apoptotic marker BCL-2 was markedly downregulated after treating the cells with ssiPD-L1 or rituximab, with effects exacerbated by combined treatment. Previous findings have also shown that overexpression of BCL-2 in DLBCL patients was closely associated with cancer aggressiveness and thus might serve as a predictor of poor outcomes in patients who received chemotherapy and immunotherapy [36]. Collectively, our results suggest that immune blockade using a PD-L1 siRNA or anti-CD20 antibody—and especially their combined application—generates an excellent inhibition of DLBCL development upon *in vitro* analysis, and we attribute the underlying mechanisms to be related to apoptosis- and NF-κB-signaling pathways.

Despite the promising findings, several limitations of this study should be acknowledged. First, although we demonstrated the functional roles of rituximab combined with PD-L1 siRNA in DLBCL cell lines, the underlying molecular mechanisms were not comprehensively investigated. Specifically, apoptosis- and NF-κB pathway-related markers were assessed only at the mRNA and protein levels, and no rescue experiments were conducted to confirm their mediating roles. Therefore, it remains possible that the observed effects represent ancillary phenomena associated with cell proliferation and death rather than direct mechanistic actions—an issue that warrants further validation through both *in vitro* and *in vivo* studies. Second, while our results revealed differential sensitivities to rituximab between SU-DHL-2 and SU-DHL-6 cells, the study lacked a non-malignant control cell line. The absence of such a control limits our ability to confirm whether the effects of the PD-L1 silencer and/or rituximab are specific to lymphoma cells. Future studies incorporating normal B cells should be conducted to address this question and further evaluate the lymphoma-specificity of this combinatorial approach. Additionally, given the heterogeneity of B-cell lymphomas—with variable PD-L1 expression across subtypes—it would be valuable in subsequent work to explore the use of a PD-L1-neutralizing antibody in place of siRNA, with the goal of identifying more clinically translatable immunotherapeutic strategies for DLBCL.

5. Conclusion

The data presented in our study provide novel insights into the contribution of PD-L1 and CD20 blockade in the development of DLBCL *in vitro*. Our data also provide initial support for the hypothesis that apoptosis-related and NF-κB-signaling pathways are crucial for enabling the PD-L1 inhibitor and anti-CD20 antibody to exert their tumor-suppressive effects, which provides a new approach for targeting PD-L1 and CD20 in the treatment of DLBCL.

Availability of Data and Materials

The data that support the findings of this study are available from the corresponding author upon reasonable request.

Author Contributions

WZ designed the research study. ZM and XP performed the research. WC analyzed the data. ZM drafted the manuscript. All authors contributed to critical revision of the manuscript for important intellectual content. All authors read and approved the final manuscript. All authors have participated sufficiently in the work and agreed to be accountable for all aspects of the work.

Ethics Approval and Consent to Participate

Not applicable.

Acknowledgment

We thank LetPub for its linguistic assistance during the preparation of this manuscript. During the experiment, Ma Hailin actively contacted the testing instruments and related laboratories.

Funding

The study was supported by the Science and Nature Foundation of Xinjiang Uyghur Autonomous Region (Grant No. 2019D01C286).

Conflicts of Interest

The authors declare no conflicts of interest.

References

[1] Li XQ, Li GD, Gao ZF, Zhou XG, Zhu XZ. The relative frequencies of lymphoma subtypes in China: A nationwide study of 10002 cases by the Chinese Lymphoma Study Group (CLSG). Annals of Oncology. 2011; 22: 141. https://doi.org/10.1093/annonc/mdr213

[2] Barraclough A, Hawkes E, Sehn LH, Smith SM. Diffuse large B-cell lymphoma. Hematological Oncology. 2024; 42: e3202. https://doi.org/10.1002/hon.3202

[3] Dunleavy K, Roschewski M, Wilson WH. Precision treatment of distinct molecular subtypes of diffuse large B-cell lymphoma: ascribing treatment based on the molecular phenotype. Clinical Cancer Research : an Official Journal of the American Association for Cancer Research. 2014; 20: 5182–5193. https://doi.org/10.1158/1078-0432.CCR-14-0497

[4] Sehn LH, Gascoyne RD. Diffuse large B-cell lymphoma: optimizing outcome in the context of clinical and biologic heterogeneity. Blood. 2015; 125: 22–32. https://doi.org/10.1182/blood-2014-05-577189
[5] Ghione P, Salles G. Spotlight on polatuzumab vedotin: new standards for diffuse large B-cell lymphoma? Haematologica. 2024; 109: 2802–2809. https://doi.org/10.3324/haematol.2022.282362
[6] Lavacchi D, Landini I, Perrone G, Roviello G, Mini E, Nobili S. Pharmacogenetics in diffuse large B-cell lymphoma treated with R-CHOP: Still an unmet challenge. Pharmacology & Therapeutics. 2022; 229: 107924. https://doi.org/10.1016/j.pharmthera.2021.107924
[7] Zhou L, Cheng W, Luo Q, Huang C, Yu L. Targeting epigenetic reprogramming in DLBCL and its interaction with the tumor microenvironment for novel therapeutic approaches. International Immunopharmacology. 2025; 161: 115012. https://doi.org/10.1016/j.intimp.2025.115012
[8] Liu Y, Zhou X, Wang X. Targeting the tumor microenvironment in B-cell lymphoma: challenges and opportunities. Journal of Hematology & Oncology. 2021; 14: 125. https://doi.org/10.1186/s13045-021-01134-x
[9] Ilcus C, Bagacean C, Tempescul A, Popescu C, Parvu A, Cenariu M, et al. Immune checkpoint blockade: the role of PD-1-PD-L axis in lymphoid malignancies. OncoTargets and Therapy. 2017; 10: 2349–2363. https://doi.org/10.2147/OTT.S133385
[10] Kiyasu J, Miyoshi H, Hirata A, Arakawa F, Ichikawa A, Niino D, et al. Expression of programmed cell death ligand 1 is associated with poor overall survival in patients with diffuse large B-cell lymphoma. Blood. 2015; 126: 2193–2201. https://doi.org/10.1182/blood-2015-02-629600
[11] Twa DDW, Chan FC, Ben-Neriah S, Woolcock BW, Mottok A, Tan KL, et al. Genomic rearrangements involving programmed death ligands are recurrent in primary mediastinal large B-cell lymphoma. Blood. 2014; 123: 2062–2065. https://doi.org/10.1182/blood-2013-10-535443
[12] Zinzani PL, Santoro A, Gritti G, Brice P, Barr PM, Kuruvilla J, et al. Nivolumab Combined With Brentuximab Vedotin for Relapsed/Refractory Primary Mediastinal Large B-Cell Lymphoma: Efficacy and Safety From the Phase II CheckMate 436 Study. Journal of Clinical Oncology : Official Journal of the American Society of Clinical Oncology. 2019; 37: 3081–3089. https://doi.org/10.1200/JCO.19.01492
[13] Chong EA, Alanio C, Svoboda J, Nasta SD, Landsburg DJ, Lacey SF, et al. Pembrolizumab for B-cell lymphomas relapsing after or refractory to CD19-directed CAR T-cell therapy. Blood. 2022; 139: 1026–1038. https://doi.org/10.1182/blood.2021012634
[14] Jain N, Senapati J, Thakral B, Ferrajoli A, Thompson P, Burger J, et al. A phase 2 study of nivolumab combined with ibrutinib in patients with diffuse large B-cell Richter transformation of CLL. Blood Advances. 2023; 7: 1958–1966. https://doi.org/10.1182/bloodadvances.2022008790
[15] Liu J, Quan L, Zhang C, Liu A, Tong D, Wang J. Over-activated PD-1/PD-L1 axis facilitates the chemoresistance of diffuse large B-cell lymphoma cells to the CHOP regimen. Oncology Letters. 2018; 15: 3321–3328. https://doi.org/10.3892/ol.2017.7682
[16] Lenz G. Novel NF-κB regulator in ABC DLBCL. Blood. 2016; 127: 2785–2786. https://doi.org/10.1182/blood-2016-03-704254
[17] Niu M, Shen Y, Xu X, Yao Y, Fu C, Yan Z, et al. Piperlongumine selectively suppresses ABC-DLBCL through inhibition of NF-κB p65 subunit nuclear import. Biochemical and Biophysical Research Communications. 2015; 462: 326–331. https://doi.org/10.1016/j.bbrc.2015.04.136
[18] Li H, Xia JQ, Zhu FS, Xi ZH, Pan CY, Gu LM, et al. LPS promotes the expression of PD-L1 in gastric cancer cells through NF-κB activation. Journal of Cellular Biochemistry. 2018; 119: 9997–10004. https://doi.org/10.1002/jcb.27329
[19] Bi XW, Wang H, Zhang WW, Wang JH, Liu WJ, Xia ZJ, et al. PD-L1 is upregulated by EBV-driven LMP1 through NF-κB pathway and correlates with poor prognosis in natural killer/T-cell lymphoma. Journal of Hematology & Oncology. 2016; 9: 109. https://doi.org/10.1186/s13045-016-0341-7
[20] Tanaka Y, Maeshima AM, Nomoto J, Makita S, Fukuhara S, Munakata W, et al. Expression pattern of PD-L1 and PD-L2 in classical Hodgkin lymphoma, primary mediastinal large B-cell lymphoma, and gray zone lymphoma. European Journal of Haematology. 2018; 100: 511–517. https://doi.org/10.1111/ejh.13033
[21] Li L, Sun R, Miao Y, Tran T, Adams L, Roscoe N, et al. PD-1/PD-L1 expression and interaction by automated quantitative immunofluorescent analysis show adverse prognostic impact in patients with diffuse large B-cell lymphoma having T-cell infiltration: a study from the International DLBCL Consortium Program. Modern Pathology : an Official Journal of the United States and Canadian Academy of Pathology, Inc. 2019; 32: 741–754. https://doi.org/10.1038/s41379-018-0193-5
[22] Gupta GK, Jaffe ES, Pittaluga S. A study of PD-L1 expression in intravascular large B cell lymphoma: correlation with clinical and pathological features. Histopathology. 2019; 75: 282–286. https://doi.org/10.1111/his.13870
[23] Chen L, Han X. Anti-PD-1/PD-L1 therapy of human cancer: past, present, and future. The Journal of Clinical Investigation. 2015; 125: 3384–3391. https://doi.org/10.1172/JCI80011
[24] Yokosuka T, Takamatsu M, Kobayashi-Imanishi W, Hashimoto-Tane A, Azuma M, Saito T. Programmed cell death 1 forms negative costimulatory microclusters that directly inhibit T cell receptor signaling by recruiting phosphatase SHP2. The Journal of Experimental Medicine. 2012; 209: 1201–1217. https://doi.org/10.1084/jem.20112741
[25] Mitteldorf C, Berisha A, Pfaltz MC, Broekaert SMC, Schön MP, Kerl K, et al. Tumor Microenvironment and Checkpoint Molecules in Primary Cutaneous Diffuse Large B-Cell Lymphoma-New Therapeutic Targets. The American Journal of Surgical Pathology. 2017; 41: 998–1004. https://doi.org/10.1097/PAS.0000000000000851
[26] Kwon D, Kim S, Kim PJ, Go H, Nam SJ, Paik JH, et al. Clinicopathological analysis of programmed cell death 1 and programmed cell death ligand 1 expression in the tumour microenvironments of diffuse large B cell lymphomas. Histopathology. 2016; 68: 1079–1089. https://doi.org/10.1111/his.12882
[27] Hamed MM, Gouida MS, Abd El-Aziz SR, El-Sokkary AMA. Evaluation PD-L1, CD8 and CD20 as early predictor and tracking markers for breast cancer (BC) in Egypt. Heliyon. 2022; 8: e09474. https://doi.org/10.1016/j.heliyon.2022.e09474
[28] Feng Y, Liu L, Li J, Huang J, Xie JH, Menard L, et al. Systematic characterization of the tumor microenvironment in Chinese patients with hepatocellular carcinoma highlights intratumoral B cells as a potential immunotherapy target. Oncology Reports. 2022; 47: 38. https://doi.org/10.3892/or.2021.8249
[29] Zhang J, Medeiros LJ, Young KH. Cancer Immunotherapy in Diffuse Large B-Cell Lymphoma. Frontiers in Oncology. 2018; 8: 351. https://doi.org/10.3389/fonc.2018.00351
[30] Ou JN, Wiedeman AE, Stevens AM. TNF-α and TGF-β counterregulate PD-L1 expression on monocytes in systemic lupus erythematosus. Scientific Reports. 2012; 2: 295. https://doi.org/10.1038/srep00295
[31] He J, Hu Y, Hu M, Li B. Development of PD-1/PD-L1 Pathway in Tumor Immune Microenvironment and Treatment for Non-Small Cell Lung Cancer. Scientific Reports. 2015; 5: 13110. https://doi.org/10.1038/srep13110
[32] D'Alterio C, Buoncervello M, Ieranò C, Napolitano M, Portella

L, Rea G, et al. Targeting CXCR4 potentiates anti-PD-1 efficacy modifying the tumor microenvironment and inhibiting neoplastic PD-1. Journal of Experimental & Clinical Cancer Research : CR. 2019; 38: 432. https://doi.org/10.1186/s13046-019-1420-8

[33] Carrà G, Lingua MF, Maffeo B, Taulli R, Morotti A. P53 vs NF-κB: the role of nuclear factor-kappa B in the regulation of p53 activity and vice versa. Cellular and Molecular Life Sciences : CMLS. 2020; 77: 4449–4458. https://doi.org/10.1007/s00018-020-03524-9

[34] Prescott JA, Mitchell JP, Cook SJ. Inhibitory feedback control of NF-κB signalling in health and disease. The Biochemical Journal. 2021; 478: 2619–2664. https://doi.org/10.1042/BCJ20210139

[35] Cippitelli M, Stabile H, Kosta A, Petillo S, Lucantonio L, Gismondi A, et al. Role of NF-κB Signaling in the Interplay between Multiple Myeloma and Mesenchymal Stromal Cells. International Journal of Molecular Sciences. 2023; 24: 1823. https://doi.org/10.3390/ijms24031823

[36] Johnson NA, Slack GW, Savage KJ, Connors JM, Ben-Neriah S, Rogic S, et al. Concurrent expression of MYC and BCL2 in diffuse large B-cell lymphoma treated with rituximab plus cyclophosphamide, doxorubicin, vincristine, and prednisone. Journal of Clinical Oncology : Official Journal of the American Society of Clinical Oncology. 2012; 30: 3452–3459. https://doi.org/10.1200/JCO.2011.41.0985